Leukemia
https://doi.org/10.1038/s41375-019-0447-3

ARTICLE

Myelodysplastic syndrome

Biology and prognostic impact of clonal plasmacytoid dendritic cells in chronic myelomonocytic leukemia

Nolwenn Lucas[1,2,3] · Matthieu Duchmann[1] · Philippe Rameau[4] · Floriane Noël[5] · Paula Michea[5] · Véronique Saada[3] · Olivier Kosmider[6,7] · Gérard Pierron[4] · Martin E Fernandez-Zapico[8,9] · Matthew T. Howard[8,9] · Rebecca L. King[8,9] · Sandrine Niyongere[10] · M'boyba Khadija Diop[1,4] · Pierre Fenaux[11] · Raphael Itzykson[11] · Christophe Willekens[1,3] · Vincent Ribrag[1,3] · Michaela Fontenay[6,7] · Eric Padron[10] · Vassili Soumelis[5] · Nathalie Droin[1,4] · Mrinal M Patnaik[12] · Eric Solary[1,2,3]

Received: 10 November 2018 / Revised: 13 February 2019 / Accepted: 11 March 2019
© Springer Nature Limited 2019

Abstract

Islands of CD123^{high} cells have been commonly described in the bone marrow of patients with chronic myelomonocytic leukemia (CMML). Using a multiparameter flow cytometry assay, we detected an excess of CD123^{+} mononucleated cells that are lineage-negative, CD45^{+}, CD11c^{-}, CD33^{-}, HLA-DR^{+}, BDCA-2^{+}, BDCA-4^{+} in the bone marrow of 32/159 (20%) patients. Conventional and electron microscopy, flow cytometry detection of cell surface markers, gene expression analyses, and the ability to synthesize interferon alpha in response to Toll-like receptor agonists identified these cells as bona fide plasmacytoid dendritic cells (pDCs). Whole-exome sequencing of sorted monocytes and pDCs identified somatic mutations in genes of the oncogenic RAS pathway in the two cell types of every patient. CD34^{+} cells could generate high amount of pDCs in the absence of FMS-like tyrosine kinase 3-ligand (FLT3L). Finally, an excess of pDCs correlates with regulatory T cell accumulation and an increased risk of acute leukemia transformation. These results demonstrate the FLT3L-independent accumulation of clonal pDCs in the bone marrow of CMML patients with mutations affecting the RAS pathway, which is associated with a higher risk of disease progression.

Introduction

Plasmacytoid dendritic cells (pDCs) are bone-marrow derived cells whose development relies mostly on Fms-like tyrosine kinase 3 ligand (FLT3L) [1] and the master transcription factor TCF4 [2]. Mature pDCs lack most of

Supplementary information The online version of this article (https://doi.org/10.1038/s41375-019-0447-3) contains supplementary material, which is available to authorized users.

✉ Mrinal M Patnaik
Patnaik.Mrinal@mayo.edu

✉ Eric Solary
eric.solary@gustaveroussy.fr

1 INSERM U1170, Gustave Roussy Cancer Center, Villejuif, France

2 Université Paris-Sud, Faculté de Médecine, Le Kremlin-Bicêtre, France

3 Department of Hematology, Gustave Roussy Cancer Center, Villejuif, France

4 INSERM US23, CNRS UMS3655 Gustave Roussy Cancer Center, Villejuif, France

5 INSERM U932, Institut Curie, PSL Research University, Paris, France

6 Inserm U1016, CNRS UMR8104, Institut Cochin, Université Paris Descartes, Paris, France

7 Hôpital Cochin, Service d'hématologie biologique, Paris, France

8 Schulze Center for Novel Therapeutics, Mayo Clinic, Rochester, MN 55905, USA

9 Department of Laboratory Medicine and Pathology, Mayo Clinic, Rochester, MN 55905, USA

10 Malignant Hematology Department, H. Lee Moffitt Cancer Center, Tampa, FL, USA

11 Department of Hematology, Hopital Saint Louis, Universite Paris Diderot, Paris, France

12 Division of Hematology, Department of Medicine, Mayo Clinic, Rochester, MN, USA

Published online: 20 March 2019

the lineage surface markers for B, T, NK cells and monocytes but express HLA-DR, CD123 (Interleukin-3 receptor alpha, IL-3Rα), CD303 (BDCA2) and CD304 (BDCA4/Neuropilin-1) [3]. These cells are the most important source of type I interferons (IFN-I) following recognition of viruses or nucleic acids through Toll-like receptor-7 (TLR7) and TLR9 [4]. They can also capture, process and present or cross-present antigens [5], bridging innate and adaptive immune response [6]. pDCs infiltrate a variety of human neoplasms [7]. In most cases, these tumor-associated pDCs are defective in IFN-I production and exert a suppressive or tolerogenic function, primarily by inducing IL-10 producing regulatory T cells [8–11].

Chronic myelomonocytic leukemia (CMML) is a myeloid malignancy associated with the age-related accumulation of somatic mutations in a hematopoietic stem or progenitor cell (HSPC) [12]. This disease associates cellular dysplasia with proliferative features including monocytosis [13]. Although not specific, the high incidence of *TET2*, *SRSF2*, *ASXL1* and signaling mutations (*NRAS, KRAS* and *CBL*) is characteristic of this disease [14, 15]. Myeloid progenitors commonly demonstrate hypersensitivity to granulocyte macrophage-colony stimulating factor (GM-CSF) [16, 17]. Median overall survival of CMML patients ranges between 15 and 30 months. Approximately 25% of these patients die from disease transformation into acute myeloid leukemia (AML) [18]. Allogeneic stem cell transplantation is a potentially curative therapeutic option [19], while cytoreductive drugs and hypomethylating agents have limited impact on long-term outcome [20].

In the 1980s, pathologists identified the presence of irregular islands of CD123-positive cells in the bone marrow and tissues of a fraction of patients with acute and chronic myeloid neoplasms, with a strong predominance in CMML [21–24]. These cells were initially described as plasmacytoid T cells because of their plasma cell-like morphology and their expression of CD4 [25], then as plasmacytoid monocytes because of their expression of monocyte markers [26]. Their precise identity, the mechanisms promoting their generation and their impact on disease evolution had not been explored thus far.

We show that $CD123^{+}$ cells infiltrating the bone marrow of CMML patients are bona fide pDCs according to the most recent classification, and belong to the leukemic clone [27, 28]. The emergence of pDC islands is preferentially observed in RAS-mutated CMML, in which stem and progenitor cell differentiation is skewed toward pDC generation in a FLT3L-independent manner. An increase in the number of pDCs correlates with an increased risk of leukemic transformation, bringing novel insights into CMML pathophysiology.

Patients and methods

Cell collection

Two cohorts of 159 (French cohort) and 202 (US cohort) patients, respectively, were studied after approval by institutional review boards. The characteristics of these cohorts are presented in Tables 1 and S1. Disease diagnosis fulfilled the WHO 2016 classification criteria [13]; cytogenetic risk was stratified according to the CMML-specific prognostic scoring system (CPSS) [29], and samples were collected after obtaining written informed consent. The French cohort was used to perform a prospective flow cytometry analysis of fresh samples and to characterize CD123-positive cells in the bone marrow and peripheral blood of CMML patients. In this cohort, sorted monocyte DNA, available on 126 (79%) patients, was subjected to a 38-gene panel targeted capture assay (Table S2). The US cohort was used to perform a retrospective immunohistochemical analysis of bone marrow trephine biopsies collected in all patients at CMML diagnosis. In this cohort (median follow-up was 81 months), bone marrow mononucleated cell (BMMC) DNA, simultaneously collected on 167 (83%) patients, was subjected to a 29-gene panel targeted capture assay (Table S2) [30]. The availability of frozen PBMC for 38 patients of this cohort allowed correlating pDC status in trephine biopsies and in peripheral blood by flow cytometry.

Flow cytometry

BMMC and peripheral blood mononucleated cells (PBMC) were incubated for 15 min at room temperature with Fc blocking reagent (Miltenyi Biotech) before being stained for 45–60 min at 4 °C with antibodies. Subsequent intracellular staining was obtained by cell fixation with Perm/Fix (BD Biosciences) for 20 min at room temperature and Perm/Wash washing before incubation with antibodies for 60 min at 4 °C. Flow analysis was performed on a BD LSRFortessa X-20 with BD FACSDiva software (BD biosciences). pDCs (Figure S1 and supplemental methods) were quantified as the fraction of PBMC or BMMC, whose count was refined using a CD33 vs. side structure (SSC) plot, which enables elimination of residual dysplastic immature myeloid cells. We used Kaluza (Beckman Coulter, Brea, California, USA) for flow analyses. We calculated the cut-off value defining an increased fraction of pDCs in mononucleated cells to be 1.2% in the bone marrow and 0.6% in the peripheral blood (see results). Antibodies and cell sorting methods are in supplemental methods.

Cell morphology and immunohistochemistry

Sorted pDCs were analyzed on May–Grunwald Giemsa stained cytospins ($n = 10$, 7 CMML and 3 controls). For

Table 1 Characteristics of chronic myelomonocytic leukemia (CMML) patients whose bone marrow mononucleated cells were prospectively analyzed by flow cytometry (French cohort) or bone marrow trephine biopsy was retrospectively analyzed by immunohistochemistry (US cohort)

	French cohort ($N = 159$)					US cohort ($N = 202$)				
Variables	*N*	All patients	pDC-rich 32 (20%)	pDC-poor 127 (80%)	*p*-value	*N*	All patients	pDC-rich 45 (22%)	pDC-poor 157 (78%)	*p*-value
General characteristics										
Median age in years [IQR]	158	74 [68–81]	78 [73–83]	74 [68–80]	0.04	202	71 [64–76]	68 [58–73]	71 [65–76]	0.005
Male number (%)	126	81 (64%)	16 (59%)	65 (66%)	NS	202	135 (67%)	32 (71%)	103 (66%)	NS
Blood cell parameters										
Hemoglobin, g/dL, median [IQR]	140	11.1 [9.4–12.9]	11.3 [9.7–12.2]	11.1 [9.2–12.9]	NS	201	10.6 [9.4–12.3]	11.3 [9.5–12.8]	10.5 [9.1–12.1]	NS
WBC × 10^9/L, median [IQR]	140	11.1 [7.0–18.9]	12.0 [8.4–24.1]	11.1 [6.7–18.6]	NS	201	12.2 [6.4–24.1]	12.2 [5.4–20.5]	12.3 [6.6–26.6]	NS
AMC × 10^9 /L, median [IQR]	140	2.4 [1.3–4.9]	2.4 [1.8–4.8]	2.4 [1.2–4.9]	NS	200	2.4 [1.2–5.1]	2.5 [1.2–5.1]	2.5 [1.2–5.1]	NS
Platelets × 10^9/L, median [IQR]	137	102 [54–191]	93 [52–187]	104 [54–197]	NS	201	97 [54–174]	96 [48–159]	99 [57–178]	NS
BM blast %, median [IQR]	127	6 [3–8]	6 [4–8]	5 [3–8]	NS	195	3 [1–6]	4 [2–7]	2 [1–5]	NS
WHO 2016 categories, number (%)										
CMML-0		53 (42%)	8 (29%)	45 (46%)			124 (64%)	24 (55%)	100 (66%)	
CMML-1	127	52 (41%)	17 (61%)	35 (35%)	NS	195	39 (20%)	10 (23%)	29 (19%)	NS
CMML-2		22 (17%)	3 (11%)	19 (19%)			32 (16%)	10 (23%)	22 (15%)	
Dysplastic	140	79 (56%)	15 (50%)	64 (58%)	NS	201	107 (53%)	24 (53%)	83 (53%)	NS
Proliferative		61 (44%)	15 (50%)	46 (42%)			94 (47%)	21 (47%)	73 (47%)	
Cytogenetic risk according to CPSS, number (%)										
Low		66 (80%)	14 (82%)	52 (80%)			139 (70%)	31 (69%)	108 (71%)	
Intermediate	82	8 (10%)	0	8 (12%)	NS	198	37 (19%)	9 (20%)	28 (18%)	NS
High		8 (10%)	3 (18%)	5 (8%)			22 (11%)	5 (11%)	17 (11%)	
Mutated gene by NGS analysis of gene panels, number (%)										
NRAS	126	24 (19%)	9 (35%)	15 (15%)	0.046	167	28 (17%)	11 (30%)	17 (13%)	0.02
KRAS	126	19 (15%)	5 (19%)	14 (14%)	NS	167	7 (4%)	3 (8%)	4 (3%)	NS
CBL	126	19 (15%)	6 (23%)	13 (13%)	NS	167	23 (14%)	9 (24%)	14 (11%)	NS
Combination of mutations detected by NGS analysis of gene panels: at least one mutation in *NRAS* or *KRAS* or *CBL* genes										
NRAS + *KRAS* + *CBL*	126	58 (46%)	18 (69%)	40 (40%)	0.014	167	56 (34%)	22 (59%)	34 (26%)	<0.001

pDC plasmacytoid dendritic cells, *N* number of samples with available information, *WHO* World Health Organization, *WBC* white blood cells, *ANC* absolute neutrophil count, *AMC* absolute monocyte count, *CMML* chronic myelomonocytic leukemia, *BM* bone marrow, *CPSS* CMML-specific prognostic scoring system, *NS* non-significant

ultrastructural studies ($n = 4$, 3 CMML and 1 control), they were fixed in 1.6% glutaraldehyde (v/v in 0.1 M phosphate buffer) and post-fixed with 2% osmium tetroxide (w/v in 0.1 M phosphate buffer). Following dehydration through a graded ethanol series, they were embedded in Epon™ 812 and ultrathin sections were stained with standard uranyl acetate and lead citrate. Images were taken using a Tecnai 12 electron microscope (FEI, Eindhoven, The Netherlands). Immunohisto-chemistry was performed on formalin-fixed and decalcified paraffin-embedded bone marrow biopsies (details in supplemental methods). pDC-rich samples were defined as those with >5% of the BM cells demonstrating a pDC morphology and expressing CD123.

pDC generation and stimulation

BMMC and PBMC (2×10^6 cells/mL) were incubated for 3 h at 37 °C with TLR agonists, to which Brefeldin A was added for three additional hours. After washing with cold PBS (Gibco), cells were stained extracellularly, fixed, permeabilized and stained intracellularly. The procedure for analysis of intracellular cytokines is detailed in the supplemental methods section. To generate pDCs, $CD34^+$ cells were cultured in X-vivo 15 (Lonza, Amboise, France) supplemented with insulin 10 ng/mL, liposomes 20 ng/mL, thrombopoietin (TPO, 50 ng/mL), stem cell factor (SCF, 50 ng/mL), FLT3L 100 ng/mL and interleukin-3 (IL-3, 20 ng/mL), prior to the flow cytometry-based detection and analysis of generated pDCs (see supplemental methods).

Cytokine measurement in bone marrow supernatants

Fresh bone marrow samples were centrifuged at $150 \times g$ for 10 min, and supernatants were collected and frozen at −80 °C until analysis using mesoscale (Meso Scale Diagnostics, Rockville, Maryland, USA) technology with two 9-plex ((IFNα, IL1Rα, FLT3L, GM-CSF, CXCL12, VEGF, TNFα, IL10 et IL17α) and (IL1β, IL6, IL8, IL4, IL2Rα, IFNγ, M-CSF, MIP-1β (CCL4), TPO) panels.

Exome and gene expression analyses

Whole-exome sequencing was performed on DNA collected from sorted bone marrow T-cells ($CD3^+$), monocytes ($CD14^+$) and pDCs (Lin^- $HLA\text{-}DR^+$ $CD123^{high}$ $CD11c^-$ $BDCA4^+$). Total RNA was isolated from sorted cells with Single Cell RNA Purification Kit (Norgen Biotek Corp, Canada). Detailed methods for RNA sequencing are in the supplemental material. Differential expression analysis was performed in samples from the same batch, using the negative binomial generalized linear model fitting and Wald statistics from DESeq2* package in R software [31]. Differentially expressed genes (DEGs) were selected from three pairwise comparisons: pDC-rich vs. pDC-poor CMML, pDC-rich CMML vs. healthy donor pDCs, and pDC-poor CMML vs. healthy donor pDCs. A multiple testing correction on p-values was applied to filter out DEGs with an adjusted p-value over 0.05 and an absolute logFoldChange over 1, then a supervised hierarchical clustering of the 13 samples of pDCs represented in a heatmap.

Statistical analyses

Given the smaller number of samples, we used non-parametric tests, including Mann–Whitney test to compare continuous variables, Fischer exact to compare categorical variables and Kendall's correlation test to compare ordinal variables. The Kaplan–Meier method was used to evaluate survival data from diagnosis to death or last follow-up. Cumulative incidence of AML transformation was computed considering death as a competing risk and univariate and multivariate analyses performed with Fine & Gray's proportional subhazards model. Multivariate analysis was performed on all variables with significant impact in univariate analyses, followed by backward stepwise selection. All statistical analyses were two-sided, retaining $p < 0.05$ as statistically significant and were deduced using STATA or Prism 7 applications.

Results

CD123-positive cells infiltrate hematopoietic tissues in a fraction of CMML patients

CD123-positive cells that form irregular nodules in the bone marrow of a fraction of CMML patients (Fig. 1a) were suggested to be pDCs. To further explore the presence of pDCs in bone marrow aspirate and peripheral blood, we set up a multiparametric flow cytometry assay to detect lineage-negative ($CD3^-$, $CD14^-$, $CD15^-$, $CD16^-$, $CD19^-$, $CD24^-$), CD33-negative and CD11c-negative mononucleated cells expressing CD45, CD123, HLA-DR, BDCA-2, BDCA-4 and CD4 (Figs. 1c and S1A). Compared to age-matched healthy donor controls (24 bone marrow and 34 peripheral blood), an increased fraction of these cells was detected in BMMC of 32/159 (20%) and PBMC of 11/106 (10%) CMML patients, respectively (Fig. 1d, e and Table 1). The cut-off value defining an increased fraction of pDCs in mononucleated cells (mean + 2 SD in age-matched control samples) was calculated to be 1.2% in the bone marrow and 0.6% in the peripheral blood (Figs. 1d, e and S2B-C). Analysis of matched BMMC and PBMC samples ($n = 106$) demonstrated that the fraction of pDCs in

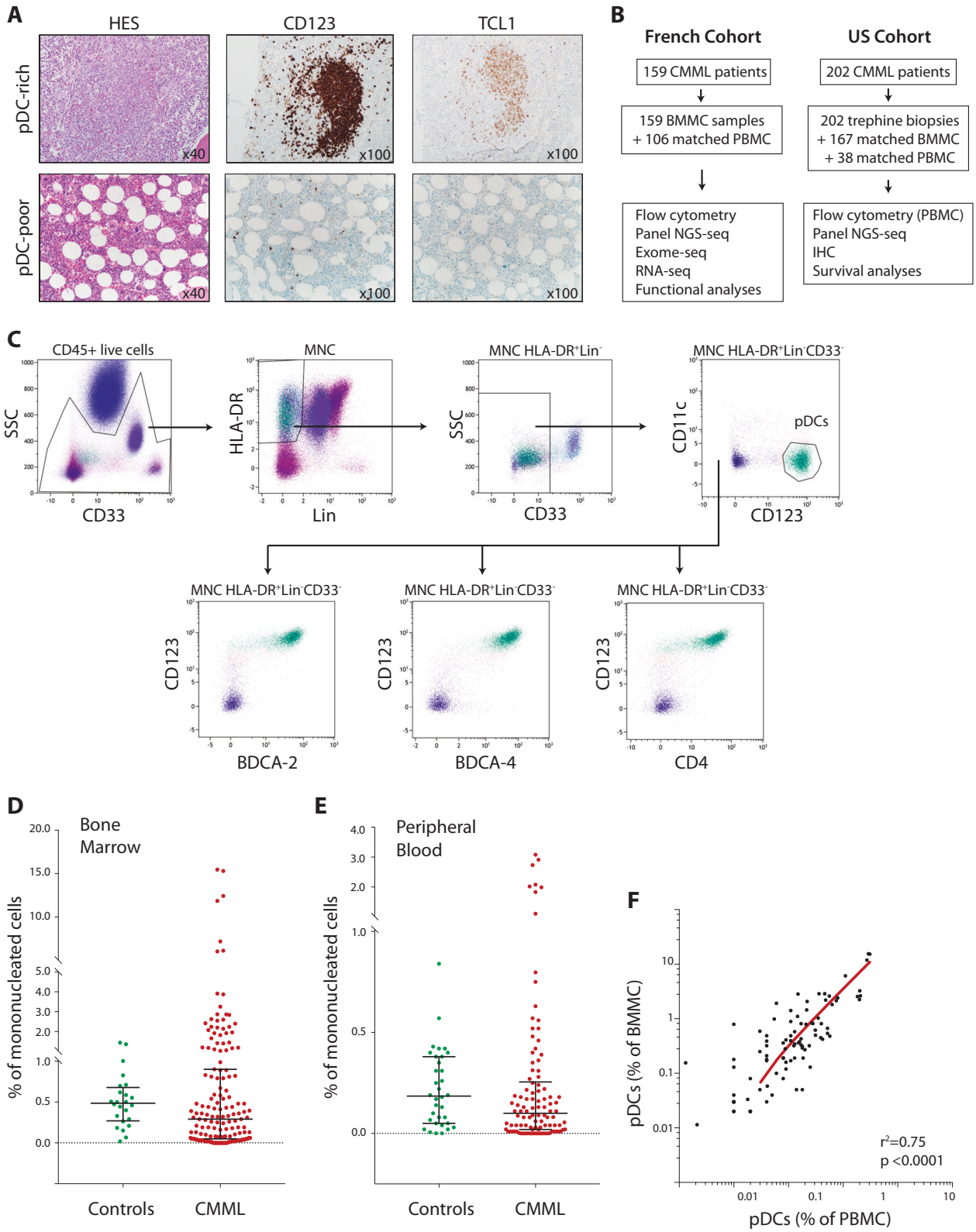

mononucleated cells was always higher in bone marrow (median %pDC 0.32 [0.04–0.81]) than in peripheral blood (0.10 [0.02–0.26]; $p < 0.0001$, Wilcoxon signed rank test, Figure S2A). Importantly, in patients whose pDC number was below the cut-off value (pDC-poor CMML patients), the fraction of pDCs was significantly lower than in healthy

◀ **Fig. 1** Identification of CD123^{high} cells in bone marrow and peripheral blood of CMML patients. **a** Histological and immunohistochemical analysis of bone marrow trephine biopsy sections of CMML patients. One CD123$^+$, TCL1$^+$ cell-rich (upper panel) and one CD123$^+$, TCL1$^+$ cell-poor (lower panel) representative cases are shown (right corner, magnification). Left column: hematoxylin/eosin staining; middle column: CD123 staining; right column: TCL1 staining. **b** Flow chart of the performed experiments in two patient cohorts. **c** Multiparameter flow cytometry analysis of pDCs in bone marrow aspirate and peripheral blood samples collected from CMML patients and age-matched healthy controls. Mononuclear cells were identified among CD45$^+$ cells using Side Scatter (SSC) and CD33 staining. pDCs were identified among mononucleated cells as HLA-DR$^+$, Lineage (CD3, CD14, CD15, CD16, CD19, CD24)$^-$, CD33$^-$, CD11c$^-$, CD123$^+$, BDCA-2$^+$, BDCA-4$^+$, CD4$^+$ cells. Green color was assigned to CD123$^+$, CD11c$^+$ cells before checking for BDCA2, BDCA4 and CD4 expression. **d**, **e** pDC richness was quantified as percentage of pDCs among mononuclear cells in bone marrow (BMMC; controls = 24, CMML = 159) (**d**) and matched peripheral blood when available (PBMC; controls = 34, CMML = 106) (**e**). **f** Linear regression of pDCs in peripheral blood, expressed as the fraction of PBMC, vs. pDCs in bone marrow, expressed as the fraction of BMMC, in the 106 CMML patients with matched samples (R^2 0.75; $p < 0.0001$)

donor tissues ($p = 0.0002$ and $p = 0.0008$ in bone marrow and peripheral blood, respectively, Figure S2B-C). Comparison of cell surface marker staining index only detected a slightly lower expression of BDCA-2 in pDC-poor CMML samples (Figure S2D-G). A significant correlation was observed between the fraction of pDCs measured in matched blood and bone marrow samples (linear regression, $R^2 = 0.75$, $p < 0.001$; Fig. 1f). This translated into a good agreement between pDC bone marrow and peripheral blood infiltration (91.5%, Cohen's kappa coefficient = 0.66). Of these 106 cases, the 11 (10%) patients with an excess of pDCs in peripheral blood had pDC excess in bone marrow, whereas 9 of the 20 patients with a pDC excess in bone marrow had a normal count in peripheral blood.

CD123-positive cells that infiltrate CMML bone marrow are bona fide pDCs

To further validate the presence of pDCs in CMML patients using a rigorous definition, we sorted CD45$^+$, Lin$^-$, HLA-DR$^+$, CD123$^+$, CD11c$^-$, BDCA-4$^+$ cells (Figure S1B) from CMML patient bone marrow and performed Giemsa staining demonstrating a typical plasma cell-like morphology that included a round or oval shape, an eccentric nucleus, basophilic cytoplasm and a pale Golgi zone known as the arcoplasm (Fig. 2a). Electron microscopic analysis of these cells showed a well-developed rough endoplasmic reticulum (RER) in an electron-dense cytoplasm (Fig. 2b) congruent with pDCs. In some cases, we also noticed cytoplasmic hyaline inclusions made of aggregates of filaments (Fig. 2b, lower panels, arrow). Flow cytometry analyses of sorted cells identified only a small fraction of cells expressing AXL and CD33 (Fig. 2c), two markers that were recently demonstrated to define independent cell populations described as pre-DC or AS/DC (AXL$^+$ SIGLEC-6$^+$ Dendritic Cell) [27, 28]. The mean fraction of contaminating pre-DCs was 3.1%, 4.1% and 0.6% of sorted cells in healthy donor, pDC-poor and pDC-rich CMML samples, respectively ($p = 0.2$, non-significant, Kruskal–Wallis test, Fig. 2d).

We then explored the ability of CMML pDCs to produce IFNα by intracellular flow cytometry analysis of mononucleated cells stimulated with TLR agonists (Fig. 2e). In the presence of brefeldin A, which induces the cytoplasmic retention of synthesized cytokines, IFNα was detected in the cytoplasm of a fraction of bone marrow (Fig. 2f) and peripheral blood (Fig. 2g) pDCs stimulated for 6 h with a TLR7 agonist (the guanosine analog loxoribine, 2 mM) or a TLR9 agonist (CpG ODN2395, 1 μM).

Since pDC accumulation in solid tumors has been associated with an expansion of regulatory T cells (Tregs), we measured the fraction of CD3$^+$, CD4$^+$, CD25^{high}, CD127^{low} Tregs (Figure S1) in BMMC and PBMC of pDC-rich and pDC-poor CMML patients, and in healthy donors. The fraction of Tregs among T cells was significantly higher in the bone marrow and peripheral blood of CMML patients compared to healthy donors (Fig. 2h, i). The fraction of Tregs among T cells was also significantly higher in the bone marrow (Fig. 2h) and peripheral blood (Fig. 2i) of pDC-rich bone marrow patients. We noticed a significant positive correlation between pDC infiltration and the fraction of Tregs measured in BMMC and PBMC, respectively (Figure S2).

CMML pDCs are close to healthy donor pDCs

RNA-sequencing was performed in pDCs sorted from pDC-rich ($n = 11$) and poor ($n = 5$) CMML bone marrow samples. Gene expression in these cells were similar to that observed in pDC sorted from age-matched healthy donors ($n = 7$) (Fig. 3a). More specifically, genes recently defined as pDC top markers [27] and those otherwise described as being highly expressed in healthy donor pDCs, including *HLA-DR, CD123, CLEC4C (*BDCA2*), TLR9, TLR7, NRP1* (BDCA4), *IRF7*, *LILRA4* (ILT7) and *TCF4* (E2.2) genes, were also highly expressed in CMML-associated pDCs. CMML-derived pDCs expressed low levels of *CD5, CD2* and *SIGLEC6* genes that characterize the recently described pre-DC [28] or "AS DC" [27] population and low levels of lineage specific genes (Fig. 3a). Of note, while *AXL* mRNA was variably expressed in all groups tested, low levels of the protein were detected by flow analysis (Fig. 2d). Principal component analysis performed on the 500 most variable genes across pDCs did not distinguish pDCs sorted from pDC-rich and pDC-poor CMML bone marrow samples and from healthy donor bone marrow (not shown). DEG

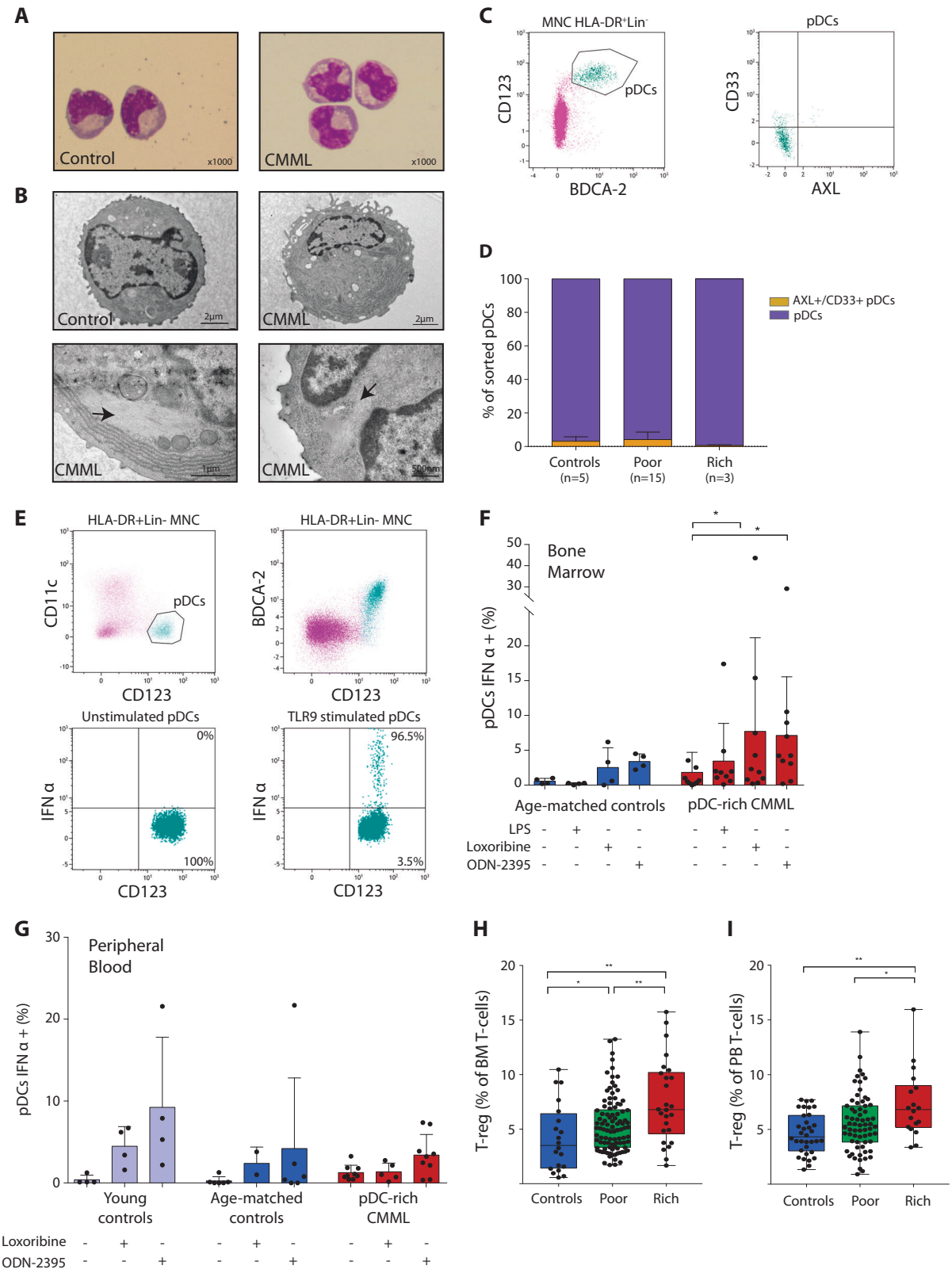

analysis focused on pDC collected from pDC-rich CMML ($n = 6$), pDC-poor CMML ($n = 3$) and healthy donor ($n = 4$) bone marrow samples detected 74 DEGs between pDC-poor and pDC-rich CMML, 13 DEGs between pDC-rich CMML and healthy-donor pDC, and 144 DEGs between pDC-poor CMML and healthy-donor pDC (Table S3).

◀ **Fig. 2** CD123$^+$ cells identified in CMML patients are bona fide plasmacytoid dendritic cells. **a** Giemsa staining of CD45$^+$, Lin$^-$, HLA-DR$^+$, CD123$^+$, CD11c$^-$, BDCA-4$^+$ sorted cells from a healthy bone marrow (left panel) or a CMML bone marrow (right panel), (right corner, magnification). **b** Transmission electronic microscopy of cells sorted as in **a**. Upper panel, left: healthy bone marrow; right: CMML bone marrow. Note the round cells, with characteristic abundant parallel rough endoplasmic reticulum. Lower panel, CMML bone marrow cells with arrows showing packed juxtanuclear bundle-shaped microfilaments. **c** Cell surface expression of "AS DC" (AXL$^+$ SIGLEC-6$^+$ Dendritic Cell) markers by cells sorted as in **a**. Note that very few cells express CD33 and AXL. **d** Fraction of AXL$^+$, CD33$^+$ cells among cells sorted as in **a**. In the following panels, "pDC-rich" indicate CMML in which the fraction of pDCs in the bone marrow was >1.2% of mononucleated cells. **e–g** Flow cytometry analysis of pDCs, gated as in Fig. 1c, expressing intracellular IFNα Representative flow cytometry analysis (**e**) and fraction of bone marrow (**f**) and peripheral blood (**g**) pDCs with intracellular IFNα when stimulated with 1 µg/ml LPS, 2 mM loxoribine and 1 µM ODN2395 for 6 h and treated with 5 µg/mL brefeldin A for the last 3 h of stimulation. *$p < 0.05$ (Wilcoxon ranked test). **h** Fraction of Treg cells (CD3$^+$, CD4$^+$, CD25^{high}, CD127^{low}) among T cells as measured by flow cytometry in BMMCs collected from 26 pDC-rich and 98 pDC-poor CMML patients and 20 healthy donors. **i** Fraction of Tregs measured by flow cytometry in PBMCs collected from 18 pDC-rich and 67 pDC-poor CMML patients and from 34 healthy donors. *$p < 0.05$; **$p < 0.01$, (Mann–Whitney test)

Supervised hierarchical clustering indicated that these genes could discriminate the three sample categories (Fig. 3b). Gene Ontology enrichment analysis performed using overrepresentation test [32, 33] demonstrated a trend toward enrichment in IFN-I signaling pathway, response to IFN-I and cellular defense response in upregulated genes in pDCs from pDC-rich compared to pDC-poor CMML (adjusted p-value = 0.11).

pDC bone marrow infiltration correlates with increased leukemic transformation

Since pDC infiltration has been associated with a poor outcome in diverse solid tumors, we hypothesized that pDC bone marrow enrichment in chronic phase CMML before any treatment may be informative on disease evolution. In the French prospective cohort, only 58 samples were collected at diagnosis, of which 13 were pDC-rich. The median follow-up was only 21.7 months, which was inappropriate to evaluate the prognostic value of pDC infiltration measured by flow cytometry, Therefore, we performed this prognostic analysis on an independent retrospective cohort of 202 patients in which pDCs were detected by immunohistopathology (Tables 1 and S1). Bone marrow was considered as "pDC-rich" when >5% of the BM cells demonstrated a pDC morphology on hematoxylin–eosin-stained samples, and were CD123$^+$ as a minimum inclusion criterion, most of them being also TCL1$^+$. Median follow-up in this cohort was 81 months. pDC infiltration measured in the peripheral blood of 38 of these patients by flow cytometry was in good accordance with immunohistochemistry analyses, i.e. pDCs over 0.6% of PBMC were detected only in patients with pDCs > 5% in the bone marrow by immunohistochemistry (Fig. 4a). pDC enrichment of CMML bone marrow was not statistically associated with overall survival outcomes, even when higher percentages of pDCs were used as cut-offs for being considered "pDC-rich" CMML (>10%, >25% and >50%) (not shown). However, pDC-rich CMML according to bone marrow immunohistochemistry was associated with a significantly higher cumulative incidence of leukemic transformation, considering death as a competing risk (Fig. 4b, standardized hazard ratio (sHR) 2.59 [95% confidence interval (CI) 1.21–5.51]; $p = 0.014$). Importantly, an increased bone marrow infiltration with pDCs remained an independent prognostic factor in multivariate analysis (sHR 3.3 [95% CI: 1.47–7.]; $p = 0.004$), together with peripheral blood blast cell count and immature myeloid cell fraction (Table S4).

Bone marrow infiltrating pDCs are detected in RAS-mutated CMML

Having demonstrated that CD123^{high} cells that accumulate in the bone marrow of 20% of patients with CMML are bona fide pDCs, we wanted to determine if their accumulation was related to specific genetic events. In the French cohort, pDC-rich CMML samples demonstrated a significantly higher incidence of mutations in *NRAS* alone, or in combination with *KRAS* and *CBL* gene mutations in their sorted monocytes (Table 1). These correlations were validated in the US cohort of 202 patients analyzed by immunohistochemistry (Table 1). Targeted sequencing analysis in sorted monocytes and sorted pDCs of two patients, identified similar genetic alterations (heterozygous mutations in *TET2* (R1261L) and *ASXL1* (G642fs) genes in sample #1723, in *TET2* (M508F and V1136fs), *SRSF2* (P95H), *CBL* (Y371H and W251X), *SETBP1* (D868N), and *ASXL1* (I901fs) in sample #1755), with similar variant allele frequencies, thus validating the fact that pDCs were an integral part of the leukemic clone. Importantly, sample #1723 was a pDC-poor CMML (0.01% pDCs in BMMCs), indicating that pDCs from both pDC-rich and pDC-poor CMML were part of the clone.

We then sorted bone marrow pDCs, peripheral blood CD14$^+$ monocytes, and CD3$^+$ T cells from 10 CMML patients. All ten cases displayed marrow pDC enrichment, thus enabling for the sorting of a sufficient amount of each cell population to perform whole-exome sequencing (Figs. 5a, S3A and Table S5). In every CMML patient, we detected at least one (five cases) and sometimes two or more (five cases) somatic mutations in genes encoding proteins of

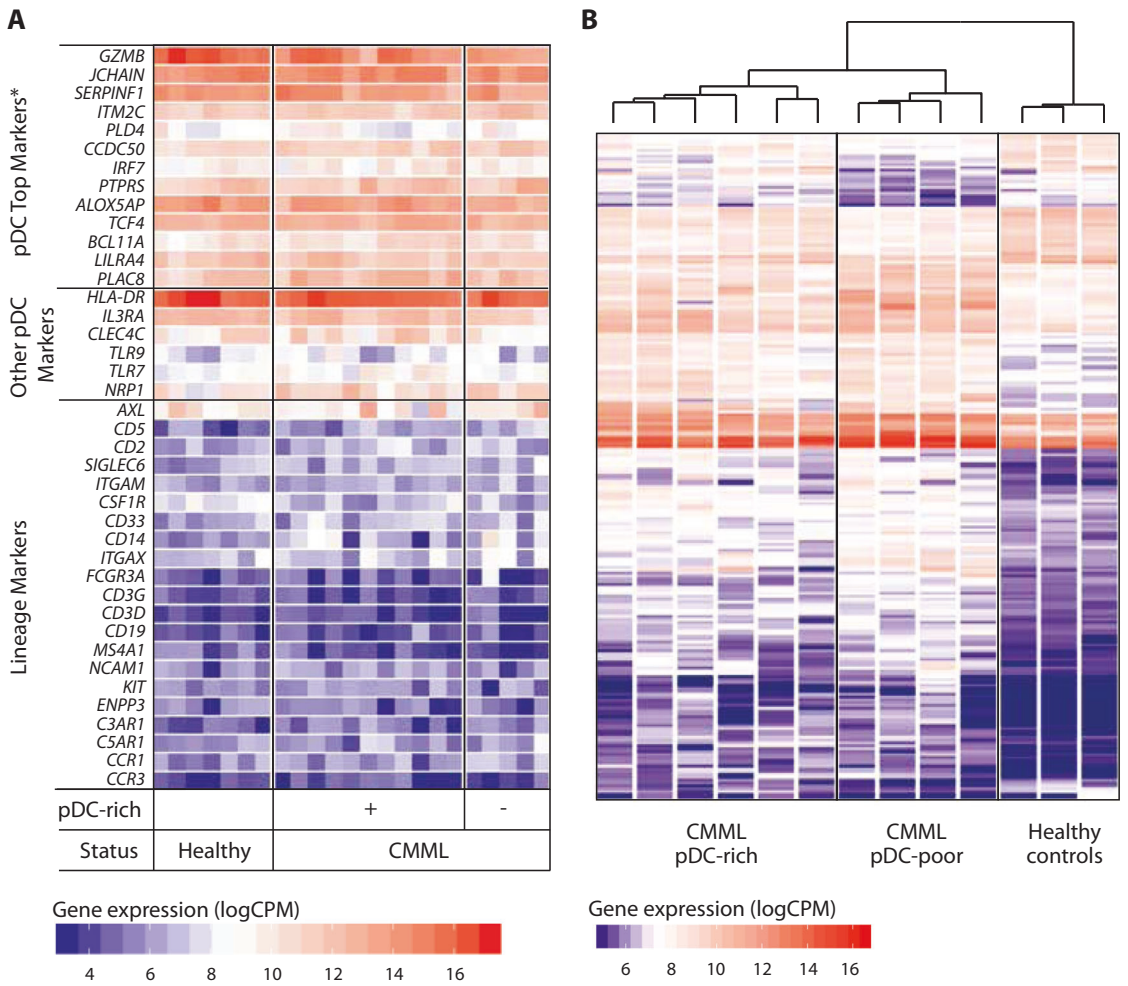

Fig. 3 Gene expression analysis validates CD123$^+$ cells as bona fide plasmacytoid dendritic cells. pDC-rich indicate CMML in which the fraction of pDCs in bone marrow mononucleated cells was >1.2%. **a** Heat-map of gene expression measured by RNA sequencing in pDCs sorted from healthy donors ($n = 7$), pDC-rich ($n = 11$) and pDC-poor ($n = 5$) bone marrow CMML samples, distinguishing genes considered as pDC top markers according to Villani et al. [27], other pDC markers and lineage markers. **b** Supervised hierarchical clustering of bone marrow pDCs, based on differentially expressed genes (DEGs) as identified by RNA sequencing in pDCs sorted from a cohort of 3 healthy donors, 6 pDC-rich CMML and 4 pDC-poor CMML bone marrow samples (The list of DEGs is provided as supplemental Table 3, pDC-poor vs, pDC-rich CMML, DEGs = 74; pDC-rich vs, healthy-donor pDCs, DEGs = 13; pDC-poor CMML vs, healthy-donor pDCs, DEGs = 144)

the RAS pathway. These heterogeneous mutations included variants in *NRAS*, *KRAS*, *NF1*, *CBL*, *PTPN11*, *MAP2K1* and *GPS2* genes (Fig. 5a). A significant correlation was observed between variant allele frequencies measured in monocytes and in pDCs (linear regression, $r^2 = 0.78$, $p < 0.0001$, Fig. 5b). Some clonal heterogeneity could be detected, e.g. in sample #2048, *NRAS*^{G13D} identified in sorted pDCs was barely detected in sorted monocytes (Fig. 5c) whereas, of the three mutations involving the RAS pathway detected in sample #1829, NRAS^{A59D} was almost exclusively identified in sorted monocytes (Fig. 5d). Finally, in one bone marrow sample (#2387), we were able to sort progenitor populations [34, 35]. This sample was collected from the same patient as sample #2062, with a 10.4-month interval between the two collection time points. Analysis of somatic mutations in sorted monocytes detected the loss of a KRAS^{G60V} subclone. Five other somatic mutations showed a similar variant allele frequency in every cell compartment (Figure S3B).

CD34$^+$ cells from pDC-rich CMML are hypersensitive to FLT3L

We then analyzed the ability of CD34$^+$ cells from CMML patients to generate pDCs in vitro by culturing these cells in the presence of SCF, TPO, IL-3 and FLT3L for 30 days [36, 37]. Serial flow analysis of CD34$^+$ cells-derived pDCs identified the fraction of CD45$^+$ live cells with a HLA-DR$^+$, Lin$^-$, CD123^{high}, CD11c$^-$, CD34$^-$, BDCA4$^+$ phenotype as pDCs (Fig. 6a). Morphological analysis of generated cells

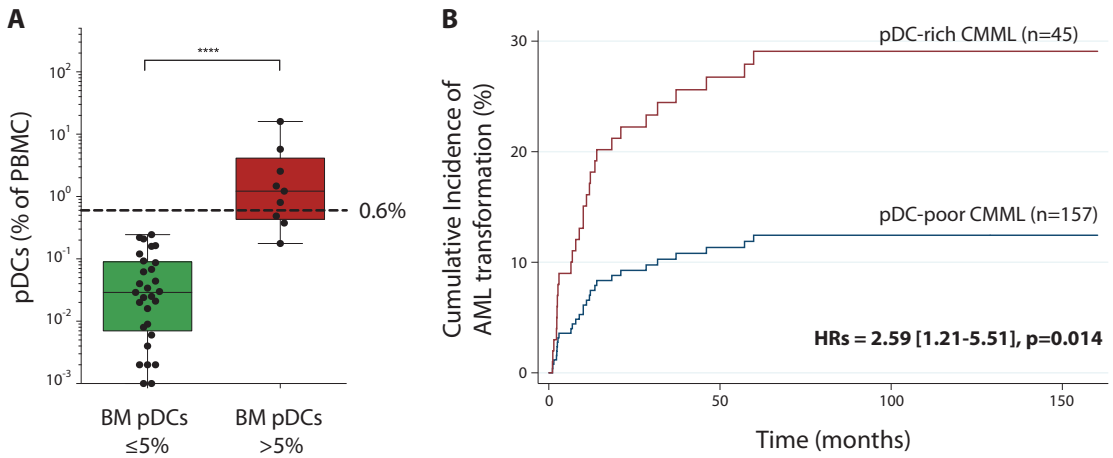

Fig. 4 pDC bone marrow infiltration correlates with an increased risk of acute leukemia transformation. **a** Relationship between immunohistochemistry analysis of bone marrow CD123$^+$ cells (pDC rich, >5% of bone marrow cells demonstrating a dendritic cell morphology and CD123 expression, most of them being also TCL1 positive) and flow cytometry measurement of pDC fraction in peripheral blood samples (pDC rich >0.6% of mononucleated cells) analyzed in 38 patients. $p < 0.001$; Mann–Whitney test. Agreement in 92% of cases, Kohen's kappa 0.75. **b** Cumulative incidence of acute myeloid leukemia transformation in 202 CMML patients according to pDC infiltration, as defined by immunohistochemistry analysis of bone marrow biopsies (pDC-rich > 5% CD123$^+$ TCL1$^+$ cells), considering death as a competing risk (hazard ratio 2.59 [95% confidence interval (CI) 1.21–5.51]; $p = 0.014$)

after sorting, using conventional microscopy (Fig. 6b, upper panel) and electron microscopy (Fig. 6b, lower panel), confirmed pDC features. From day 15 to day 25, the number of pDCs generated by CD34$^+$ cells collected from pDC-rich CMML bone marrow was increased as compared with healthy donor and pDC-poor samples (Fig. 6c, d). Analysis of somatic variants detected the same abnormalities with similar allele frequencies in sorted fresh pDCs and pDCs generated in culture from CD34$^+$ cells (Figure S4). We repeated the experiments in the absence or presence of increasing amount of FLT3L, demonstrating the ability of CD34$^+$ cells from pDC-rich CMML to produce pDCs in the absence of FLT3L and to produce more pDCs in response to low concentrations of FLT3L (Fig. 6e). Interestingly, FLT3-L level was decreased in CMML patients, and this decrease was significantly more important in pDC-rich CMML (Fig. 6f). Of the 18 other cytokines whose level was measured in marrow plasma, only TPO and TGF-beta levels were decreased in CMML compared to healthy donor bone marrow plasma, without significant difference between pDC-rich and pDC-poor CMML (Figure S5).

Discussion

The current study indicates that ~20% of CMML patients demonstrate an increased number of bona fide pDCs in their bone marrow. Somatic mutations in genes of the oncogenic RAS pathway were detected in all the pDC-rich patients and their CD34$^+$ cells could differentiate into pDCs in the absence of FLT3L. pDC amplification in the leukemic clone correlates with a higher rate of regulatory T cells in the bone marrow and peripheral blood, and a higher risk of AML transformation.

The presence of CD123$^+$ cell islands in the bone marrow of a fraction of patients has long been identified in CMML and other myeloid neoplasms [23, 38, 39]. This pathologic finding is distinct from blastic plasmacytoid dendritic cell neoplasms (BPDCN), a rare clonal proliferation of pDC precursors that affects elderly people and involves alterations in *MYC, RB1* and *IKAROS* gene family members [39]. CD56, which is typically expressed by pDC precursors that accumulate in BPDCN [39, 40], was not identified on CMML-associated morphologically mature pDCs. In addition, genetic alterations commonly encountered in BPDCN were not detected by whole-exome sequencing of sorted CMML-associated pDCs [41], and none of the studied CMML patients developed a typical BPDCN.

Because of their plasmacytoid morphology, CD123^{high} cells that infiltrate the bone marrow of CMML patients were considered as pDCs, but a definitive proof of their identity was missing. While CD123^{high} cell populations are more complex than initially thought, our study establishes the fact that most of CD123^{high} cells that accumulate in CMML bone marrows are *bona fide* pDC.

pDCs that accumulate in the bone marrow of CMML patients belong to the leukemic clone, as somatic variants identified in these cells were also detected in monocytes. In two large international cohorts, the presence of *NRAS* mutations was significantly more frequent in pDC-rich compared to pDC-poor CMML patients, with whole-exome sequencing of sorted cell subsets confirming that pDC expansion was associated with one or more mutations in genes of the oncogenic RAS pathway. Our prior analyses

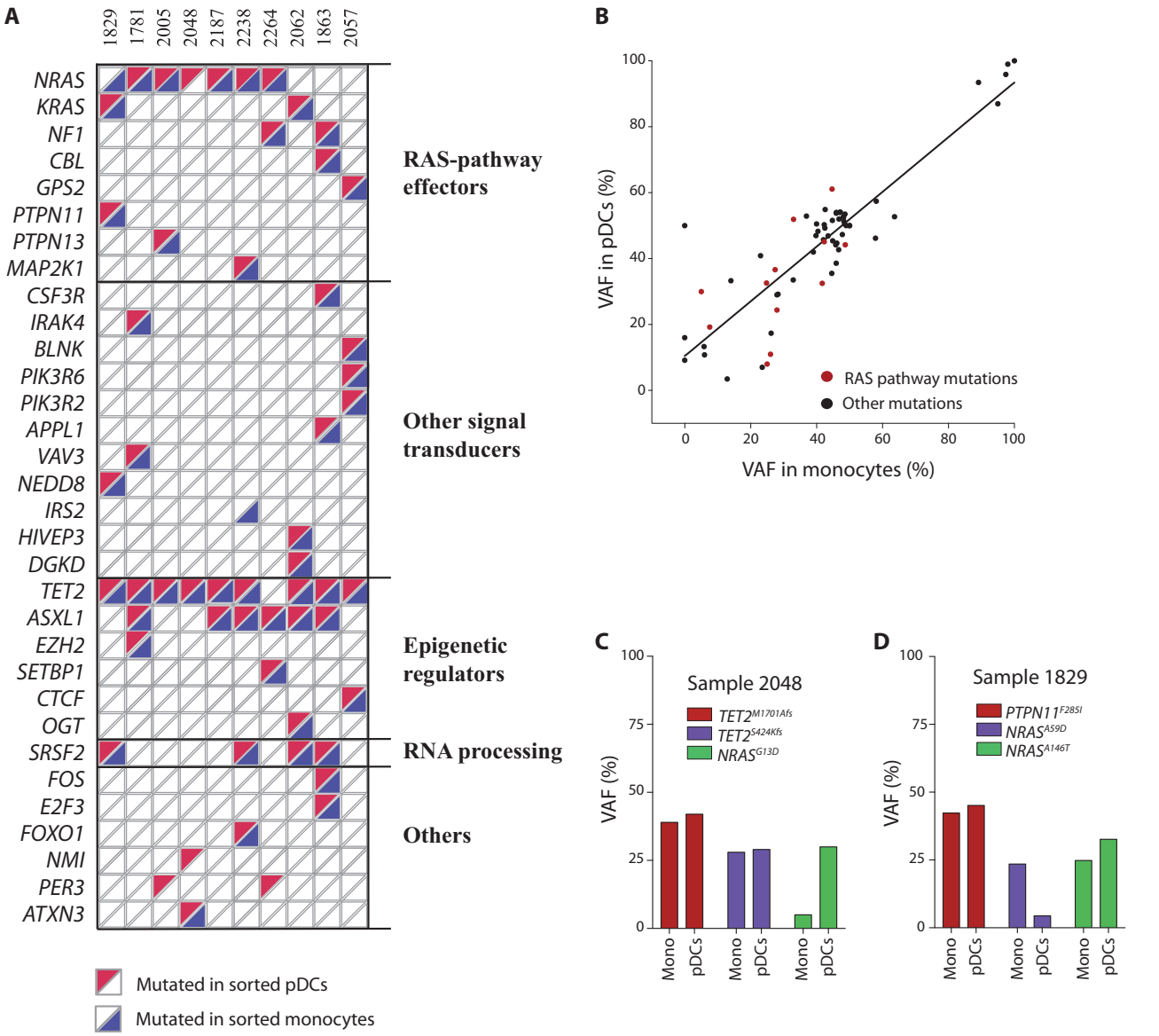

Fig. 5 Bone marrow infiltrating pDCs are observed in RAS-pathway mutated CMML. **a** Whole-exome sequencing was performed in monocytes, T cells and pDCs sorted from ten CMML bone marrow samples. Most mutations were found in both pDCs (red, left upper corner) and monocytes (blue, right lower corner). In all cases, one or more mutations in genes encoding proteins of the RAS pathway were identified in patient cells. In all but one case, these mutations were identified in both monocytes and pDCs. **b** Relationship between variant allele frequencies (VAF) measured in sorted monocytes and sorted pDCs from the ten samples sequenced in **a** (linear regression, $r^2 = 0.78$; $p < 0.0001$). RAS pathway mutations are in red, other variants in black. **c** VAF of two *TET2* gene mutations and *NRAS*^{G13D} mutation in sorted pDCs and monocytes of patient #2048. **d** VAF of *PTPN11*^{F285I}, *NRAS*^{A59D} and *KRAS*^{A146T} mutation in sorted pDCs and monocytes of patient #1829

suggested that *TET2/NRAS* double-mutant clones expand over time, including at relapse after allogeneic stem cell transplantation [16]. Studies in mice also demonstrated the cooperative effect of *NRAS* mutation and *TET2* deletion in activating the RAS signaling pathway to promote clonal expansion and leukemic progression [42]. Finally, *NRAS* mutations were shown to be part of so-called type-1 mutations associated with faster progression of MDS to AML [43]. Whether or not pDC accumulation is involved in the increased risk of AML transformation associated with RAS pathway mutations needs to be elucidated.

A concerted effect of FLT3L and GM-CSF on myeloid cell homeostasis has been described [44], with FLT3L supporting the development of pDCs through TCF4 and IRF8 and GM-CSF antagonizing this effect through STAT5 activation [45]. In patients with pDC accumulation, CD34$^+$ cells may escape the regulatory functions of these cytokines. Interestingly, pDC accumulation in a bone marrow

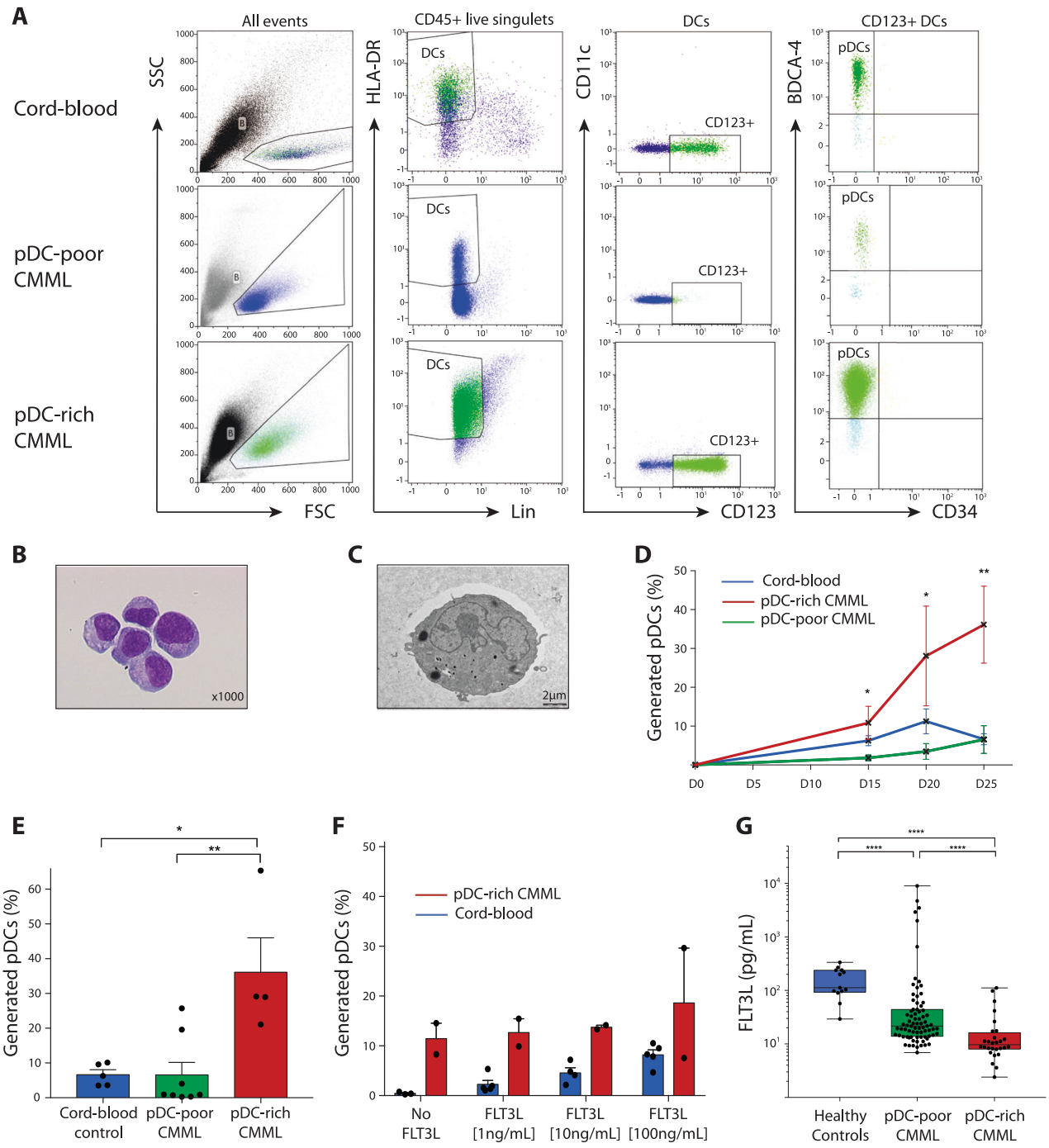

environment that produces low levels of FLT3L [46] appears to be unique among myeloid malignancies [47].

pDCs are the main type I IFN-producing cells [48]. IFNα has demonstrated antineoplastic effects through the activation of pDCs, cytotoxic T-cells and NK cells, while demonstrating a context-dependent effect on CD4 T cells [49]. IFNα has also demonstrated therapeutic benefits in myeloid malignancies [50], suggesting that stimulation of pDCs that accumulate in CMML bone marrow could have therapeutic benefits. Induction of an immune cell death of leukemic cells, e.g. with an oncolytic virus [51], could potentially activate the tumor antigen cross-presentation function and IFNα production by pDC in excess. However, pDCs that accumulate in aggressive human tumors are usually IFN-α-deficient. They promote the expansion of disease-associated Tregs, which contribute to tumor immune tolerance and poor clinical outcome [52]. Similar to high-risk MDS where disease progression correlates with an expansion of $CD4^+$ Tregs [53–55], pDC accumulation in CMML could generate an immunosuppressive environment

◀ **Fig. 6** $CD34^+$ cells from pDC-rich CMML generate pDCs in the absence of FLT3L. pDC-rich CMML were defined as in Fig. 3. **a–d** Sorted $CD34^+$ cells were cultured in the presence of SCF, TPO, FLT3L and IL-3 for indicated times before flow analysis of generated cells. **a** Representative flow cytometry detection of pDCs at day 25 of $CD34^+$ cell culture, based on HLA-DR, CD123 and BDCA4 expression. $CD34^+$ cells were collected from healthy donor cord blood (upper panel), pDC-poor (middle panel) and pDC-rich (lower panel) CMML bone marrow. **b** Generated pDCs were sorted and examined by conventional microscopy. **c** Generated pDCs were sorted and examined by electron microscopy. **d** Time-dependent generation of pDCs by ex vivo culture of $CD34^+$ cells sorted from five healthy donor cord blood (in blue), four pDC-rich (in red) and eight pDC-poor (in green) CMML bone marrow samples. The fraction of pDCs generated in culture was calculated as the fraction of $CD45^+$ live cells with a HLA-DR^+, Lin^-, $CD123^{high}$, $CD11c^-$, $CD34^-$, $BDCA4^+$ phenotype (mean ± SEM; * $P < 0.05$, Mann–Whitney test). **e** Fraction of pDCs among total mononucleated cells generated at day 25 of ex vivo culture of $CD34^+$ cells sorted from samples shown in **c** and **d** (mean ± SEM; * $P < 0.05$, Mann–Whitney test). **f** Fraction of pDCs among total mononucleated cells generated by $CD34^+$ cells sorted from two pDC-rich CMML bone marrow (in red) and five cord blood samples (in blue) and cultured for 30 days as above with increasing concentrations of FLT3L. **g** FLT3L level was measured in bone marrow supernatant of 28 pDC-rich (red) and 78 pDC-poor (green) CMML patients compared to 13 age-matched healthy controls (blue). Boxes: median, interquartiles and ranges; *** $P < 0.001$; **** $P < 0.0001$ (Mann–Whitney test)

by promoting the expansion of CD4+ Tregs, which may account for the higher risk of progression to AML. Of note, in spite of a slight correlation between the two cell populations, pDC accumulation may not be the only parameter to promote Treg expansion as these cells are also increased in so-called "pDC-poor" CMML samples, in comparison to healthy donor bone marrows.

Regardless of their biological effects, given their association with leukemic transformation, pDCs in CMML patients could serve as critical therapeutic targets. Current options include SL-401 (Tagraxofusp), an antibody conjugate targeting CD123, currently undergoing phase II trials in CMML, with preliminary data demonstrating a 71% spleen response rate and a 17% BM complete remission rate [56, 57], or with lenalidomide, an immunomodulatory drug that decreases pDC number by inducing the proteosomal degradation of Ikaros Family Zinc Finger 1 (IKZF1) transcription factor [58].

Acknowledgements This work was supported by grants from the Ligue Nationale Contre le Cancer (Equipe Labellisée), the National Cancer Institute (INCa PL-BIO and PRT-K calls), the Molecular Medicine in Oncology program supported by the Agence Nationale de la Recherche, and the SIRIC SOCRATE program. NL was supported by a grant from the Ligue Nationale Contre le Cancer, MD by the ITMO Cancer (Plan cancer 2014–2019). Part of high-throughput sequencing was performed by the genomic platform of the Institut Curie, which is supported by grants ANR-10-EQPX-03 and ANR10-INBS-09-08 from the Agence Nationale de la Recherche (Investissements d'Avenir) and by Cancéropole Ile de France. We are grateful to Sylvain Baulande and Patricia Legoix-Ne from the genomic platform of Curie Institute and Karine Bailly from the Cochin Institute cytometry and immunobiology facility for their technical support, and to Abdelkrim Achibet from the orthopedic surgery department from the hospital of Le Mans for providing us with bone marrow controls.

Author contributions NL and MD collected the samples and performed the experiments, PR set up and performed flow analyses, FN and PM analyzed the RNA sequencing data, VS and OK performed conventional microscopy, GP the electron microcopy analysis, MEFZ, MTH and RLK the immunohistochemistry, SN and EP measured FLT3L in bone marrow plasma, MKD analyzed the whole-exome sequencing data, PF, RI, CW, VR and MF provided patient samples, ND supervised the genomic analyses, MD performed the statistical analyses, ES wrote the manuscript, MF, VS and MMP corrected the manuscript, MMP and ES supervised the whole project.

Compliance with ethical standards

Conflict of interest The authors declare that they have no conflict of interest.

Publisher's note: Springer Nature remains neutral with regard to jurisdictional claims in published maps and institutional affiliations.

References

1. Waskow C, Liu K, Darrasse-Jèze G, Guermonprez P, Ginhoux F, Merad M, et al. FMS-like tyrosine kinase 3 is required for dendritic cell development in peripheral lymphoid tissues. Nat Immunol. 2008;9:676.
2. Cisse B, Caton ML, Lehner M, Maeda T, Scheu S, Locksley R, et al. Transcription factor E2-2 is an essential and specific regulator of plasmacytoid dendritic cell development. Cell. 2008;135:37–48.
3. Guilliams M, Ginhoux F, Jakubzick C, Naik SH, Onai N, Schraml BU, et al. Dendritic cells, monocytes and macrophages: a unified nomenclature based on ontogeny. Nat Rev Immunol. 2014;14:571–8.
4. Siegal FP, Kadowaki N, Shodell M, Fitzgerald-Bocarsly PA, Shah K, Ho S, et al. The nature of the principal type 1 interferon-producing cells in human blood. Science. 1999;284:1835–7.
5. Villadangos JA, Young L. Antigen-presentation properties of plasmacytoid dendritic cells. Immunity. 2008;29:352–61.
6. Kadowaki N, Antonenko S, Lau JY, Liu YJ. Natural interferon alpha/beta-producing cells link innate and adaptive immunity. J Exp Med. 2000;192:219–26.
7. Vermi W, Soncini M, Melocchi L, Sozzani S, Facchetti F. Plasmacytoid dendritic cells and cancer. J Leukoc Biol. 2011;90:681–90.
8. Zou W, Machelon V, Coulomb-L'Hermin A, Borvak J, Nome F, Isaeva T, et al. Stromal-derived factor-1 in human tumors recruits and alters the function of plasmacytoid precursor dendritic cells. Nat Med. 2001;7:1339–46.
9. Wei S, Kryczek I, Zou L, Daniel B, Cheng P, Mottram P, et al. Plasmacytoid dendritic cells induce CD8+ regulatory T cells in human ovarian carcinoma. Cancer Res. 2005;65:5020–6.
10. Conrad C, Gregorio J, Wang Y-H, Ito T, Meller S, Hanabuchi S, et al. Plasmacytoid dendritic cells promote immunosuppression in ovarian cancer via ICOS costimulation of Foxp3+ T-tegulatory cells. Cancer Res. 2012;72:5240–9.
11. Demoulin S, Herfs M, Delvenne P, Hubert P. Tumor microenvironment converts plasmacytoid dendritic cells into immunosuppressive/tolerogenic cells: insight into the molecular mechanisms. J Leukoc Biol. 2013;93:343–52.

12. Deininger MWN, Tyner JW, Solary E. Turning the tide in myelodysplastic/myeloproliferative neoplasms. Nat Rev Cancer. 2017;17:425–40.
13. Arber DA, Orazi A, Hasserjian R, Thiele J, Borowitz MJ, Beau MML, et al. The 2016 revision to the World Health Organization classification of myeloid neoplasms and acute leukemia. Blood. 2016;127:2391–405.
14. Itzykson R, Kosmider O, Renneville A, Gelsi-Boyer V, Meggendorfer M, Morabito M, et al. Prognostic score including gene mutations in chronic myelomonocytic leukemia. J Clin Oncol. 2013;31:2428–36.
15. Merlevede J, Droin N, Qin T, Meldi K, Yoshida K, Morabito M, et al. Mutation allele burden remains unchanged in chronic myelomonocytic leukaemia responding to hypomethylating agents. Nat Commun. 2016;7:10767.
16. Itzykson R, Kosmider O, Renneville A, Morabito M, Preudhomme C, Berthon C, et al. Clonal architecture of chronic myelomonocytic leukemias. Blood. 2013;121:2186–98.
17. Padron E, Painter JS, Kunigal S, Mailloux AW, McGraw K, McDaniel JM, et al. GM-CSF–dependent pSTAT5 sensitivity is a feature with therapeutic potential in chronic myelomonocytic leukemia. Blood. 2013;121:5068.
18. Patnaik MM, Tefferi A. Chronic myelomonocytic leukemia: 2016 update on diagnosis, risk stratification, and management. Am J Hematol. 2016;91:631–42.
19. de Witte T, Bowen D, Robin M, Malcovati L, Niederwieser D, Yakoub-Agha I, et al. Allogeneic hematopoietic stem cell transplantation for MDS and CMML: recommendations from an international expert panel. Blood. 2017;129:1753–62.
20. Solary E, Itzykson R. How I treat chronic myelomonocytic leukemia. Blood. 2017;130:126–36.
21. Chen Y-C, Chou J-M, Ketterling RP, Letendre L, Li C-Y. Histologic and immunohistochemical study of bone marrow monocytic nodules in 21 cases with myelodysplasia. Am J Clin Pathol. 2003;120:874–81.
22. Vermi W, Facchetti F, Rosati S, Vergoni F, Rossi E, Festa S, et al. Nodal and extranodal tumor-forming accumulation of plasmacytoid monocytes/interferon-producing cells associated with myeloid disorders. Am J Surg Pathol. 2004;28:585–95.
23. Orazi A, Chiu R, O'Malley DP, Czader M, Allen SL, An C, et al. Chronic myelomonocytic leukemia: the role of bone marrow biopsy immunohistology. Mod Pathol. 2006;19:1536–45.
24. Harris NL, Demirjian Z. Plasmacytoid T-zone cell proliferation in a patient with chronic myelomonocytic leukemia. Histologic and immunohistologic characterization. Am J Surg Pathol. 1991;15:87–95.
25. Müller-Hermelink HK, Stein H, Steinmann G, Lennert K. Malignant lymphoma of plasmacytoid T-cells. Morphologic and immunologic studies characterizing a special type of T-cell. Am J Surg Pathol. 1983;7:849–62.
26. Facchetti F, de Wolf-Peeters C, Mason DY, Pulford K, Van den Oord JJ, Desmet VJ. Plasmacytoid T cells. Immunohistochemical evidence for their monocyte/macrophage origin. Am J Pathol. 1988;133:15.
27. Villani A-C, Satija R, Reynolds G, Sarkizova S, Shekhar K, Fletcher J, et al. Single-cell RNA-seq reveals new types of human blood dendritic cells, monocytes, and progenitors. Science. 2017;356:eaah4573.
28. See P, Dutertre C-A, Chen J, Günther P, McGovern N, Irac SE, et al. Mapping the human DC lineage through the integration of high-dimensional techniques. Science. 2017;356:eaag3009.
29. Such E, Germing U, Malcovati L, Cervera J, Kuendgen A, Porta MGD, et al. Development and validation of a prognostic scoring system for patients with chronic myelomonocytic leukemia. Blood. 2013;121:3005–15.
30. Patnaik MM, Lasho TL, Vijayvargiya P, Finke CM, Hanson CA, Ketterling RP, et al. Prognostic interaction between ASXL1 and TET2 mutations in chronic myelomonocytic leukemia. Blood Cancer J. 2016;6:e385.
31. Love MI, Huber W, Anders S. Moderated estimation of fold change and dispersion for RNA-seq data with DESeq2. Genome Biol. 2014;15:550.
32. Boyle EI, Weng S, Gollub J, Jin H, Botstein D, Cherry JM, et al. GO::TermFinder--open source software for accessing Gene Ontology information and finding significantly enriched Gene Ontology terms associated with a list of genes. Bioinformatics. 2004;20:3710–5.
33. Yu G, Wang L-G, Han Y, He Q-Y. clusterProfiler: an R package for comparing biological themes among gene clusters. OMICS. 2012;16:284–7.
34. Lee J, Breton G, Aljoufi A, Zhou YJ, Puhr S, Nussenzweig MC, et al. Clonal analysis of human dendritic cell progenitor using a stromal cell culture. J Immunol Methods. 2015;425:21.
35. Lee J, Breton G, Oliveira TYK, Zhou YJ, Aljoufi A, Puhr S, et al. Restricted dendritic cell and monocyte progenitors in human cord blood and bone marrow. J Exp Med. 2015;212:385–99.
36. Chen W, Antonenko S, Sederstrom JM, Liang X, Chan ASH, Kanzler H, et al. Thrombopoietin cooperates with FLT3-ligand in the generation of plasmacytoid dendritic cell precursors from human hematopoietic progenitors. Blood. 2004;103:2547–53.
37. Demoulin S, Roncarati P, Delvenne P, Hubert P. Production of large numbers of plasmacytoid dendritic cells with functional activities from CD34+ hematopoietic progenitor cells: use of interleukin-3. Exp Hematol. 2012;40:268–78.
38. Pardanani A, Reichard KK, Zblewski D, Abdelrahman RA, Wassie EA, et al. CD123 immunostaining patterns in systemic mastocytosis: differential expression in disease subgroups and potential prognostic value. Leukemia. 2016;30:914–8.
39. Tzankov A, Hebeda K, Kremer M, Leguit R, Orazi A, van der Walt J, et al. Plasmacytoid dendritic cell proliferations and neoplasms involving the bone marrow: Summary of the workshop cases submitted to the 18th Meeting of the European Association for Haematopathology (EAHP) organized by the European Bone Marrow Working Group, Basel 2016. Ann Hematol. 2017;96:765–77.
40. Pagano L, Valentini CG, Grammatico S, Pulsoni A. Blastic plasmacytoid dendritic cell neoplasm: diagnostic criteria and therapeutical approaches. Br J Haematol. 2016;174:188–202.
41. Menezes J, Acquadro F, Wiseman M, Gómez-López G, Salgado RN, Talavera-Casañas JG, et al. Exome sequencing reveals novel and recurrent mutations with clinical impact in blastic plasmacytoid dendritic cell neoplasm. Leukemia. 2014;28:823–9.
42. Kunimoto H, Meydan C, Nazir A, Whitfield J, Shank K, Rapaport F, et al. Cooperative epigenetic remodeling by TET2 loss and NRAS mutation drives myeloid transformation and MEK inhibitor sensitivity. Cancer Cell. 2018;33:44–59.e8.
43. Makishima H, Yoshizato T, Yoshida K, Sekeres MA, Radivoyevitch T, Suzuki H, et al. Dynamics of clonal evolution in myelodysplastic syndromes. Nat Genet. 2017;49:204–12.
44. Kingston D, Schmid MA, Onai N, Obata-Onai A, Baumjohann D, Manz MG. The concerted action of GM-CSF and Flt3-ligand on in vivo dendritic cell homeostasis. Blood. 2009;114:835–43.
45. Esashi E, Wang Y-H, Perng O, Qin X-F, Liu Y-J, Watowich SS. The signal transducer STAT5 inhibits plasmacytoid dendritic cell development by suppressing transcription factor IRF8. Immunity. 2008;28:509–20.
46. Niyongere S, Lucas N, Zhou J-M, Sansil S, Pomicter AD, Balasis ME, et al. Heterogeneous expression of cytokines accounts for clinical diversity and refines prognostication in CMML. Leukemia. 2018. https://doi.org/10.1038/s41375-018-0203-0.

47. Desterke C, Bilhou-Nabéra C, Guerton B, Martinaud C, Tonetti C, Clay D, et al. FLT3-mediated p38–MAPK activation participates in the control of megakaryopoiesis in primary myelofibrosis. Cancer Res. 2011;71:2901–15.
48. Zitvogel L, Galluzzi L, Kepp O, Smyth MJ, Kroemer G. Type I interferons in anticancer immunity. Nat Rev Immunol. 2015; 15:405–14.
49. Touzot M, Grandclaudon M, Cappuccio A, Satoh T, Martinez-Cingolani C, Servant N, et al. Combinatorial flexibility of cytokine function during human T helper cell differentiation. Nat Commun. 2014;5:3987.
50. Kiladjian J-J, Giraudier S, Cassinat B. Interferon-alpha for the therapy of myeloproliferative neoplasms: targeting the malignant clone. Leukemia. 2016;30:776–81.
51. Achard C, Guillerme J-B, Bruni D, Boisgerault N, Combredet C, Tangy F, et al. Oncolytic measles virus induces tumor necrosis factor-related apoptosis-inducing ligand (TRAIL)-mediated cytotoxicity by human myeloid and plasmacytoid dendritic cells. Oncoimmunology. 2016;6:e1261240.
52. Sisirak V, Faget J, Gobert M, Goutagny N, Vey N, Treilleux I, et al. Impaired IFN-α production by plasmacytoid dendritic cells favors regulatory T-cell expansion that may contribute to breast cancer progression. Cancer Res. 2012;72:5188–97.
53. Kordasti SY, Ingram W, Hayden J, Darling D, Barber L, Afzali B, et al. CD4+CD25 high Foxp3+ regulatory T cells in myelodysplastic syndrome (MDS). Blood. 2007;110:847–50.
54. Kotsianidis I, Bouchliou I, Nakou E, Spanoudakis E, Margaritis D, Christophoridou AV, et al. Kinetics, function and bone marrow trafficking of CD4+CD25+FOXP3+ regulatory T cells in myelodysplastic syndromes (MDS). Leukemia. 2008;23:510–8.
55. Kittang AO, Kordasti S, Sand KE, Costantini B, Kramer AM, Perezabellan P, et al. Expansion of myeloid derived suppressor cells correlates with number of T regulatory cells and disease progression in myelodysplastic syndrome. Oncoimmunology. 2016;5:e1062208.
56. Patnaik MM, Gupta V, Schiller G, Lee S, Yacoub A. Results From ongoing phase 1/2 trial of SL-401 in patnient with relapsed/refractroy CMML. 2018. European Hematology Association Meeting, Stockholm.
57. Ray A, Das DS, Song Y, Macri V, Richardson P, Brooks CL, et al. A novel agent SL-401 induces anti-myeloma activity by targeting plasmacytoid dendritic cells, osteoclastogenesis and cancer stem-like cells. Leukemia. 2017;31:2652–60.
58. Cytlak U, Resteu A, Bogaert D, Kuehn HS, Altmann T, Gennery A, et al. Ikaros family zinc finger 1 regulates dendritic cell development and function in humans. Nat Commun. 2018;9. https://doi.org/10.1038/s41467-018-02977-8.